

## Relaxation, Incubation, and Dissociation in CO<sub>2</sub><sup>†</sup>

Saumitra Saxena and John H. Kiefer\*

Department of Chemical Engineering, University of Illinois at Chicago, Chicago, Illinois 60680

Robert S. Tranter

Argonne National Laboratory, Argonne, Illinois 60439

Received: October 12, 2006; In Final Form: December 18, 2006

The dissociation and relaxation of CO<sub>2</sub> has been reexamined in the incident shock wave with the laser-schlieren technique. These new experiments covered 1377–6478 K, and 42–750 Torr, and improvements partly described herein have permitted accurate determination of both rate and incubation time. In general the steady rate measurements are in agreement with other recent determinations. The one anomaly is that the new rates are not fully second order; they vary about 50% over 70–600 Torr. This unexpected feature is actually quite consistent with the recent literature, which shows a similar trend. However, attempts to produce this result with RRKM calculations were unsuccessful. Relaxation times are in agreement with available literature, and incubation time to relaxation time ratios lie between 1.5 and 3 over 4000–6600 K, consistent with findings for other molecules. These ratios are much smaller than those recently derived from reflected-shock experiments by Oehlschlaeger et al. (*Z. Phys. Chem.* **2005**, *219*, 555). A simple argument suggests such large values are indeed anomalous, although why they are too large is not clear.

### Introduction and Background

The dissociation of carbon dioxide, CO<sub>2</sub> + (M) → CO + O + (M) {1}, has a very large  $\Delta H_{298}^\circ = 127.12$  kcal/mol,<sup>1</sup> and an even larger barrier arising from the need to cross to a triplet surface<sup>2,3</sup> to reach the O(<sup>3</sup>P) ground state product. The triplet states add another 5.9 kcal/mol<sup>4</sup> to the barrier resulting in an  $E_0 = 131.59$  kcal/mol.

With such a large barrier, the thermal reaction can only be seen in the shock tube, and a fairly large number of studies have now been done this way.<sup>5–19</sup> These have employed various methods: IR emission/absorption,<sup>5–14</sup> single-pulse product analysis, SPST,<sup>15</sup> laser schlieren, LS,<sup>16</sup> O-atom ARAS,<sup>17,18</sup> and UV absorption of the CO<sub>2</sub>.<sup>19</sup> All these have involved various dilutions in rare gases, but a few studies have actually been carried out in the pure gas.<sup>20–22</sup>

A problem with many of the earlier experiments is an anomalously low  $E_a$ , even as low as 70 kcal/mol, now believed to be a consequence of rapid secondary loss of CO<sub>2</sub> via the abstraction O + CO<sub>2</sub> → CO + O<sub>2</sub> {2}, when this is catalyzed by H-atom through H + CO<sub>2</sub> → CO + OH, and OH + O → H + O<sub>2</sub>.<sup>23</sup> In recent efforts this problem has been resolved, and reasonable apparent activation energies greater than 100 kcal/mol have been obtained. In future consideration we will confine our discussion to these current examples.<sup>16–19</sup>

Vibrational relaxation in CO<sub>2</sub> is none too fast, and has been widely observed, at high temperatures, most notably by Simpson,<sup>24–27</sup> using LS and interferometry. The early concern over whether all modes relax serially, i.e., with a single relaxation time, has now been resolved<sup>28</sup> positively, and the process may be considered well understood. The relaxation measurements indicate it should be possible to observe incuba-

tion delay times,<sup>29</sup> defined as the delay in the onset of a steady dissociation reaction until vibrational energy accumulates sufficiently through relaxation after shock-heating of the cold gas. In fact, theoretical predictions of incubation delay times for CO<sub>2</sub> have been proposed in two instances,<sup>30,31</sup> and times like these should be easily observable. Most recently Oehlschlaeger et al.<sup>19</sup> have presented incubation times measured in the reflected shock, observing UV absorption of the CO<sub>2</sub>. The times they derive are quite long, about an order-of-magnitude greater than the cited theory,<sup>30,31</sup> and there are some rather simple reasons to believe they are indeed much too long (see the Results and Discussion Section). The extraction of incubation times using the alternative LS method in the incident shock, is the primary motivation for this work.

The dissociation of CO<sub>2</sub> was already studied by one of us (JHK) some years ago<sup>17</sup> using the LS method, but no incubation times were reported. The pressures used were too high for a good resolution of relaxation, and it was also felt that the LS time origin location was too uncertain for accurate determination of incubation times. Since then the LS time-origin location has been treated and reasonable accuracy established both through theory<sup>32</sup> and experiment.<sup>33</sup> In addition, the experimental resolution and sensitivity have been much improved in the intervening 32 years, so that accurate rate constants, relaxation and incubation times, are easily determined.

### Experimental Section

The essentials of the LS method and our experimental apparatus have been presented many times,<sup>34,35</sup> and only the recent improvements will be discussed here. Recently a number of changes and improvements have been made to the experiment which have resulted in improved sensitivity, time resolution and reduced noise. The changes can be considered in two parts. The first concerns the data acquisition hardware and software and the second the detector hardware.

<sup>†</sup> Part of the special issue "James A. Miller Festschrift".

\* Corresponding author. E-mail: kiefer@uic.edu.

The old data acquisition system<sup>34</sup> included a LeCroy model 2256AS digitizer and memory with 8 bit resolution and a maximum data acquisition rate of 20 MHz that could capture up to 1024 points ( $\sim 50 \mu\text{s}$ ) including pre-trigger data. The data were downloaded to a PC AT for analysis. This system proved to be a stable workhorse for many years producing high quality data; however, the 8 bit vertical resolution and 50 ns time resolution put constraints on how accurately rapid signal changes could be captured. An additional problem was encountered with maintaining and upgrading the system as components aged and began to fail. Thus, the data acquisition system was completely rebuilt around a GAGE Applied Compuscope 12100 PCI board installed in a desktop computer. At the time of purchase, the Compuscope 12100 was one of the faster boards available from GAGE and could capture a single channel at 100 MHz with 12 bit vertical resolution or two channels simultaneously at 50 MHz, thereby providing greatly improved resolution and sensitivity to small, rapid changes in the acquired signal. Furthermore, up to 1MB of data can be acquired. Although not necessary for the usual LS experiment, it is of great benefit when trouble shooting the system and examining the stability of the laser and detector. To take full advantage of the Compuscope board, a control program was written using LabView 5.1 and integrated with a data analysis and management program written in Visual Basic 6.0. This approach has simplified the management of the laboratory data, making it simple to modify the analysis codes to add additional functions, e.g., Blythe-Blackman corrections for vibrational relaxation,<sup>33</sup> and made the upgrade to different Compuscope boards a trivial matter.

The second aspect of the experiment that has been changed is the detector circuitry and housing. The actual detector is a UDT-SPOT-9D quadrant photodiode which is the same photodiode that has been used in this lab for many years. The circuitry originally developed for this device used video amplifiers. These open-loop amplifiers provide adequate bandwidth, but lack a means to implement a feedback network to fine-tune their gain and bandwidth. The redesigned circuitry uses much lower-noise high-speed operational amplifiers, implemented with time response-optimized low-pass filters, that yield less than 1% variation in gain and bandwidth for all quadrants. Additionally, in the original circuitry the two left quadrants of the detector were tied together and the two right quadrants were tied together, effectively making a photodiode with a split into halves, and outputs were provided for the left half minus the right half (L-R), used to measure deflection of the laser beam, and the two halves added (SUM) to measure the total light intensity on the photodiode. In the current design, the quadrants are all independently amplified and then additional circuitry is used to provide the L-R and SUM signals. In addition, a top-bottom output is provided that is extremely useful for vertical centering of the beam on the detector at the start of an experiment. Outputs for each quadrant are provided and these are used to check the gain and output of each quadrant for troubleshooting.

The gases were pure CO<sub>2</sub> (99.8%, Matheson) and Kr (Spectra Gases research grade), used without further purification, and mixed in a 50L glass tank with a Teflon-coated magnetic stirrer. Mixtures of 10% and 20% CO<sub>2</sub> were used herein. Molar refractivities were 6.645 for CO<sub>2</sub> and 6.367 for Kr,<sup>36</sup> and assumed constant. Ideal gas, ideal incident shock properties for complete relaxation, but with frozen chemistry, were calculated using the Burcat and Ruscic<sup>1</sup> thermodynamic data.

TABLE 1: Summary of Experiments

	$T_2$ , K	$P_2$ , Torr	$k$ , cm <sup>3</sup> mol <sup>-1</sup> s <sup>-1</sup>	$t_i$ , $\mu\text{s}$	$\tau$ , $\mu\text{s}$
20% CO <sub>2</sub> /Kr	1850	440			3.2
	2232	358			2.9
	2435	317			3.1
	3204	42			22.5
	3484	320			2.2
	3550	333			1.9
	4163	190	2.13E + 09	9.28	3.3
	4432	166	3.75E + 09	11.1	3.5
	4860	148	1.05E + 10	9.83	3.8
	5046	143	2.00E + 10	9.1	2.8
	5057	183	1.59E + 10	7.4	4.2
	5086	125	2.32E + 10	9.1	4.1
	5229	121	2.72E + 10	9.4	3.3
	5426	163	3.55E + 10	6.9	5.1
	5671	96	4.59E + 10	9.5	4.1
	5788	140	7.69E + 10	6.5	4.7
	6083	118	1.24E + 11	6.3	6.1
	6478	82	1.62E + 11	9.3	1.9
	4584	350	5.48E + 09		
	4596	340	4.82E + 09		
	5161	326	1.53E + 10		
	5281	380	1.95E + 10		
	5514	430	2.16E + 10		
	5841	379	4.31E + 10		
5962	341	5.55E + 10			
6084	432	7.37E + 10			
4108	713	7.09E + 08			
4194	665	1.14E + 09			
4364	596	1.95E + 09			
10% CO <sub>2</sub> /Kr	1377	242			10.4
	1463	223			10.9
	1670	198			10.5
	1980	160			10.1
	2304	125			10.3
	2718	94			13.0
	2812	82			12.9
	3040	71			13.8
	3518	120			6.8
	3825	177			3.3
	4536	750	3.21E + 09		
	4867	684	8.46E + 09		
	5099	604	1.10E + 10		
	5296	538	1.46E + 10		
	5512	668	2.34E + 10		
	5808	585	3.62E + 10		
5831	581	4.17E + 10			
6088	507	6.69E + 10			

Unrelaxed temperatures and densities (used in the calculation of density change through relaxation) were found with constant trans/rot heat capacities of the CO<sub>2</sub> and Kr. A complete listing of relaxed, but again chemically frozen conditions, for all the experiments, is offered in Table 1.

## Results and Discussion

**Relaxation.** Examples with nearly pure relaxation gradients are shown in Figure 1. In all such cases, the relaxation is very closely exponential, as was also seen in the earlier work of Simpson.<sup>24-27</sup> It is somewhat surprising to see accurately exponential behavior at extreme temperatures, where the large relaxing heat capacity of the CO<sub>2</sub> induces a significant temperature drop during relaxation. This does not much affect the actual relaxation time, which is not strongly dependent on temperature, but does alter the density ratio and thus the time compression in the incident shock. It seems these must be compensating effects here. With such a nicely exponential relaxation, it is a simple matter to extract precise relaxation times, and our derived results for the energy relaxation time,  $P\tau$ , as defined through

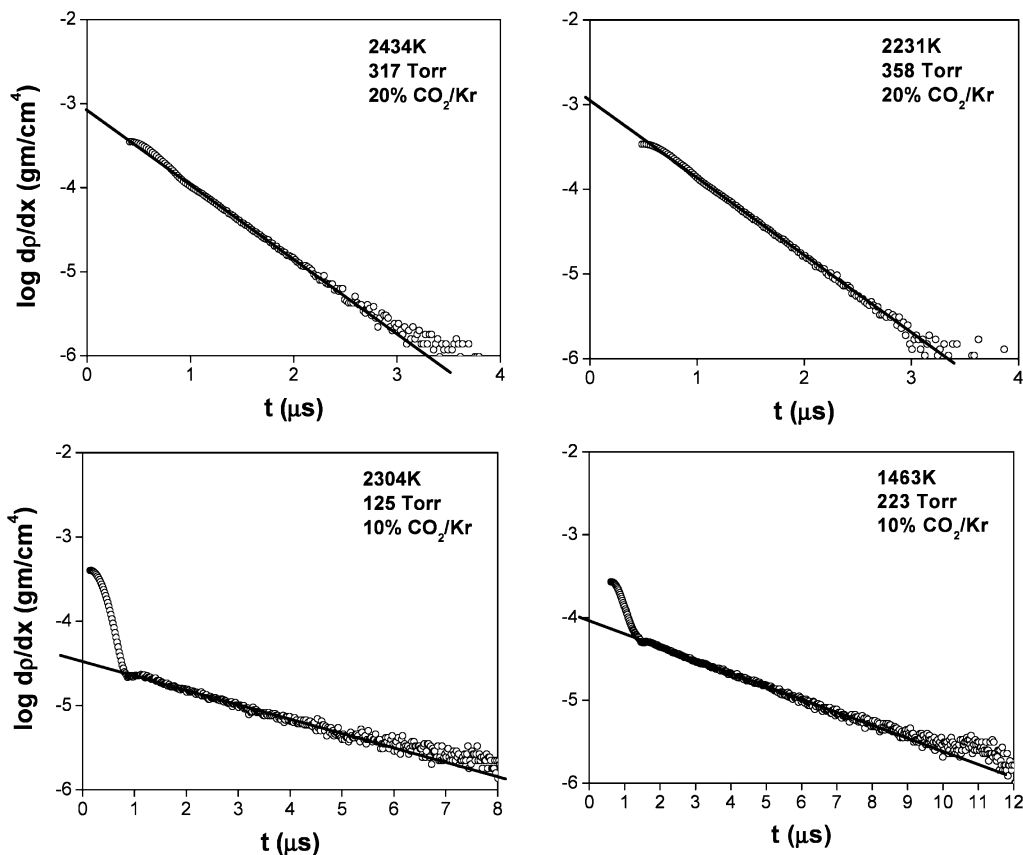


**Figure 1.** Semilog plots of laser-schlieren gradients for pure relaxation in CO<sub>2</sub>/Kr mixtures. The open circles [O] are the measurements and the solid line shows a linear fit. The first few rapidly falling points arise from beam-shock front interaction.

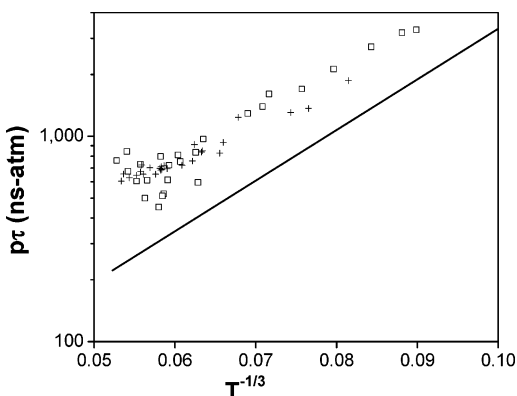


**Figure 2.** Landau–Teller plot of vibrational relaxation times for 10% CO<sub>2</sub>/Kr [□], 20% CO<sub>2</sub>/Kr [+], and extrapolation of Simpson et al.,<sup>26</sup> 10% CO<sub>2</sub>/Ar (—).

the Bethe–Teller relation,<sup>37</sup> are shown in Figure 2 and again listed in Table 1.

These  $P\tau$  values are obtained from the raw slopes of the semilog LS profiles, transforming from lab to molecule time (density ratio), and finally correcting from density to energy relaxation with the very accurate Blackman–Blythe procedure described previously.<sup>35</sup> All properties used in the derivation of relaxation times were assumed to be vibrationally relaxed conditions. If the relaxation time does not vary during relaxation, as here, this simplification should be quite appropriate.

An extrapolation of Simpson's results for  $P\tau$  in 10% CO<sub>2</sub>/Ar<sup>26</sup> is included with the present data in Figure 2. The present relaxation times are consistently larger than these, as shown, but have a very similar  $T$ -dependence. The slight difference is

to be expected given the larger mass of Kr. Relaxation commonly shows a significant collision-partner effect, one which is not, however, usually carried over to high-temperature dissociation (vide infra).

The results in Figure 2 seem to exhibit an unexpected, perhaps anomalous, rise of  $P\tau$  at the highest temperatures. We would suggest this simply reflects the increase in vibrational heat capacity, or better, equilibrium vibrational energy, for such extreme temperatures. When this equilibrium energy becomes very large, it requires more time for it to relax, and the relaxation time accordingly lengthens.<sup>34</sup> This effect can be easily seen by calculating an effective  $\langle \Delta E \rangle_{\text{down}}$  from the measured  $P\tau$ , which removes the vibrational energy and the collision frequency from the problem.<sup>33</sup> Such calculated  $\langle \Delta E \rangle_{\text{down}}$  are shown in Figure 3, where it is seen the anomalous  $T$ -dependence has now disappeared. Thus, the slight rise of  $P\tau$  at the highest temperatures is not an anomaly and might have been anticipated.

A potentially useful test of relaxation experiments with the LS method is the comparison of integrated gradients,  $\Delta\rho(\text{exp})$ , with calculated total changes in density from no vibration to vibrational equilibrium using available thermo properties,  $\Delta\rho(\text{thermo})$ . This comparison was also made in the above cited work on neopentane<sup>33</sup> and other hydrocarbons. Calculated ratios,  $\Delta\rho(\text{exp})/\Delta\rho(\text{thermo})$  are shown in Figure 4 for those experiments considered to be pure relaxation. As in the earlier effort, these ratios are somewhat too high, with an average value of about 1.5. This may seem large, but it actually arises from about a 0.1–0.2  $\mu\text{s}$  error in time origin. The reason for this error is not fully understood, although it may well arise from distributed initiation over the extensively curved shock at low pressures.

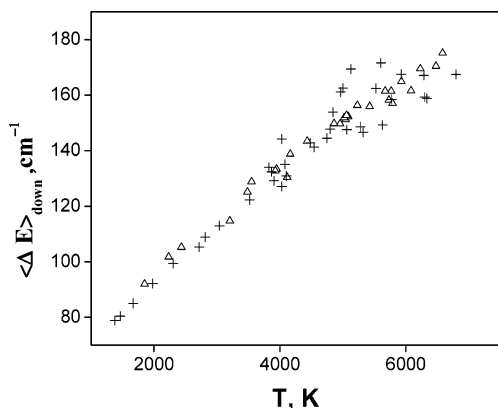


**Figure 3.** Values for  $\langle \Delta E \rangle_{\text{down}}$  derived from relaxation times for 10% CO<sub>2</sub>/Kr [+] and 20% CO<sub>2</sub>/Kr [Δ]. See text.

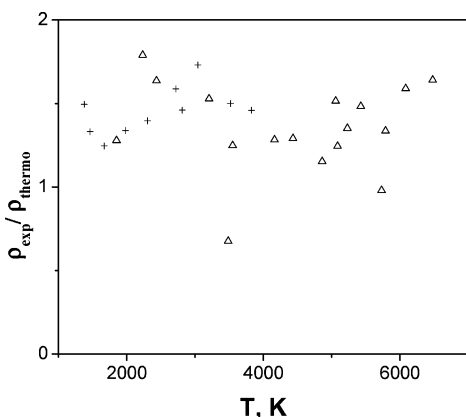


**Figure 4.** Ratios of integrated density change from experiment to thermodynamic theory,  $\Delta\rho(\text{exp})/\Delta\rho(\text{thermo})$ , for 10% CO<sub>2</sub>/Kr + and 20% CO<sub>2</sub>/Kr [Δ]. See text.

In any case this problem has been recognized for some time<sup>33,39</sup> and its behavior is entirely consistent with numerous other studies done recently using the LS technique.

**Incubation.** Example LS profiles showing both relaxation and dissociation are given in Figure 5.

Features of the process well illustrated here are: First, note how accurately the relaxation follows an exponential curve even when followed by dissociation. Second, there is a rather abrupt transition from relaxation to dissociation, marked by the arrow located at the presumed start of steady dissociation. The time to this point is now the incubation delay time,  $t_i$ .

Those of these experiments that still show well-resolved relaxation gradients were included among the listed and plotted relaxation times. In general, experiments used for more than a single observable have these all listed together in Table 1.

For a somewhat narrow region of  $T$  and  $P$ , all three observables: relaxation time, incubation delay time, and dissociation rate, can be accurately extracted. In the remaining examples of Table 1, it was considered prudent to extract only one of these three.

Measured incubation times are also listed in Table 1 and plotted in Figure 6, where we have included the new results presented by Oehlschlaeger et al.<sup>19</sup> As previously,<sup>35</sup> these times are here presented as the “time ratio,”  $t_i/\tau$ . The Oehlschlaeger et al. ratios were obtained using an extrapolation of Simpson’s relaxation times<sup>26</sup> for the same composition.

The above time ratio,  $t_i/\tau$ , has a simple and useful physical interpretation, which may be seen through the following

argument. The energy relaxation time in the denominator is obtained by fitting the Bethe–Teller relaxation equation

$$dE_{\text{vib}}/dt = (E_{\text{vib}}^{\text{eq}} - E_{\text{vib}})/\tau$$

to the observed gradients. For closely exponential relaxation, as herein, we may then integrate this as

$$E_{\text{vib}} = E_{\text{vib}}^{\text{eq}}[1 - \exp(-t/\tau)]$$

At  $t_i$ , the onset of steady dissociation

$$E_{\text{vib}} = E_{\text{vib}}^{\text{eq}}[1 - \exp(-t_i/\tau)]$$

This energy, per molecule, is now closely maintained throughout the following steady dissociation. At least for an uncomplicated single dissociation reaction, the time ratio thus measures the fractional depletion,  $1 - E_{\text{vib}}/E_{\text{vib}}^{\text{eq}} = \exp(-t_i/\tau)$ , of the vibrational energy during steady reaction.

When we apply the above to the data of Table 1, the LS results produce depletions of 3–26%, whereas the depletion suggested by the Oehlschlaeger et al.<sup>19</sup> results is effectively zero. Because their results do not agree with our LS findings and because it is physically unreasonable to have no depletion during second-order dissociation, we suggest that their incubation times must be regarded as anomalous. The long times in ref 19 are also far from the two available theories<sup>30,31</sup> which actually suggest times rather close to the LS measurements. The reasons for the problem with the ref 19 incubation times remain obscure; we can find no flaw in their methods or their experiments, but their incubation times seem much too large.

**Dissociation.** Examples of LS experiments designed to produce accurate dissociation rates are presented in Figure 7. These semilog plots of gradient also show the fit achieved by integrating a simple mechanism of just a few reactions equivalent to the two steps {1} and {2}, the latter with the rate given by Eng et al.<sup>40</sup> A few reactions of H-atom, at a reasonable impurity level (40 ppm), were often included to test their possible catalytic acceleration of reaction {2}, but in all cases, these and reaction {2} itself were of no consequence to the gradient. Of course the primary reason for this is the near thermoneutrality of {2} at high  $T$ , whether catalyzed or not, inasmuch as  $\Delta H^\circ$  for {2} is less than 3 kcal/mol for present dissociation temperatures. Thus, the contribution of this reaction to the density gradient is quite insignificant regardless of its rate. This feature is part of what makes the LS technique so nearly ideal for the study of this reaction, as was pointed out in the earlier LS work.<sup>16</sup> To produce the excellent fits in Figure 7, only the magnitude and activation energy of the second-order rate constant for {1}, here denoted  $k_d$ , were actually varied.

In the high-pressure examples of the dissociation group in Table 1, the relaxation is barely detected and the incubation time is short. For these, then, only dissociation rates can safely be obtained. However, as noted, all observables that can reasonably be derived from each experiment are listed in Table 1.

The derived  $k_d$  are all presented in the Arrhenius plot of Figure 8. In this figure one sees that the LS results show a surprising variation with pressure. Included with these are those of the “current” studies selected earlier. On the whole the LS experiments are near the earlier work but only closely agree with these when they are compared at similar pressures. The quite unexpected observation here is that the wide range of pressures

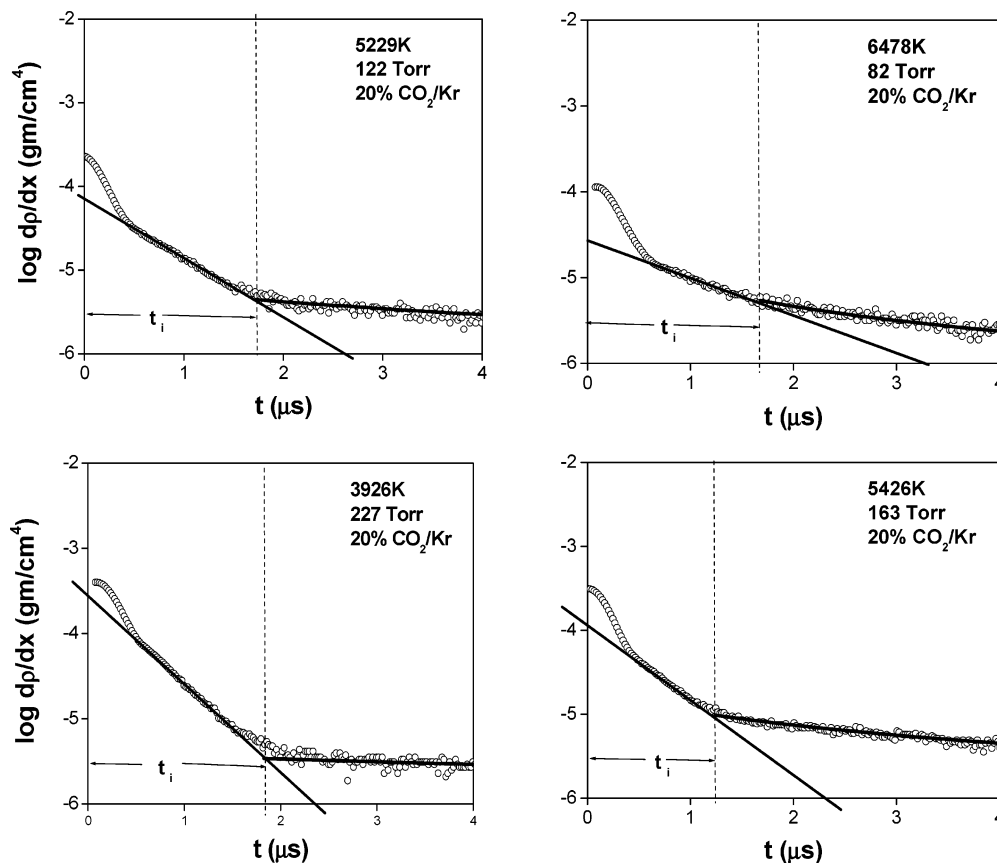


**Figure 5.** Semilog LS profiles showing relaxation, incubation, and dissociation. Note caption of Figure 1. The steep straight lines at the outset are linear fits of the initial exponential relaxation and the subsequent curves show modeling of the following steady reaction. The  $t_i$  are incubation times, here bounded by vertical dashed lines.

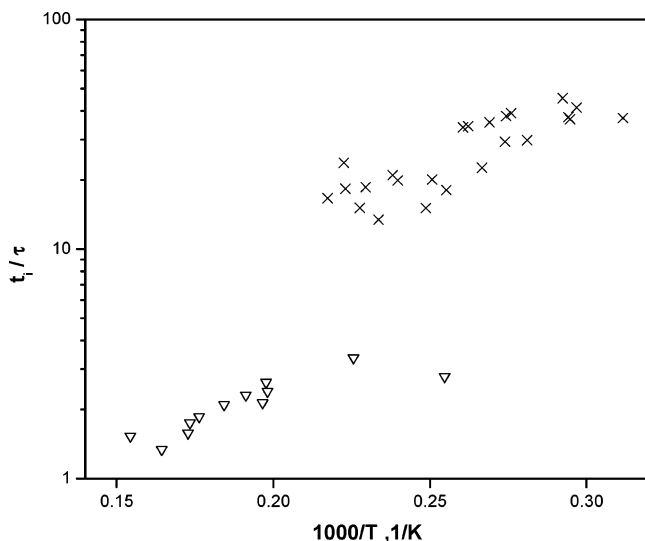


**Figure 6.** Incubation to relaxation time ratios,  $t_i/\tau$ , from present work in 20%  $\text{CO}_2/\text{Kr}$  ( $\nabla$ ) and from Oehlschaeger et al. for  $\text{CO}_2$  dilute in Ar ( $\times$ ). The Oehlschaeger et al. ratios were obtained by dividing their incubation times by relaxation times taken from Simpson et al.<sup>26</sup> for identical conditions.

offered by the LS experiments suggests that this reaction is not fully second-order even at the present extreme temperatures and moderate to low pressures. Note that this notion is actually quite consistent with the selected “current” literature data, which also rises fairly consistently with decreasing pressure. In fact, despite the rather narrow spread of pressure in the literature data, a quite consistent drop in second-order rate with pressure is still discernible, as shown in the fixed- $T$  plot of Figure 9.

Of course there are other differences among the selected studies in Figures 8 and 9 besides pressure. The LS results are for Kr, the others in Ar, and there are also wide variations in the fraction of  $\text{CO}_2$ . Differing compositions might well alter such second-order rate constants. However, it seems unlikely that small fractions of reactant would have much effect, given that the pure  $\text{CO}_2$  experiments of refs 21 and 22 provide rates very close to the present rare-gas values. Also, by now a number of studies of high-temperature unimolecular rates<sup>41</sup> have exhibited little difference between Kr and Ar collision efficiencies. Again, note that our Kr rates are quite close to the Ar rates of ref 19 when compared at similar pressures.

The origin of this residual falloff is certainly not evident to the authors. It is clearly inconsistent with the high-pressure falloff reported by Wagner and Zabel.<sup>14</sup> We have performed our own Gorin-model RRKM<sup>42</sup> fit to this data (see Table 2 and Figure 10)—Wagner and Zabel used RRK—and with this model and the experimental conditions of Figure 8, our calculations indicate a deviation from second order over 50–760 Torr of 5% or less, almost too small to notice, whereas our experiments indicate a drop of the second-order rate nearer 40% for this increase in pressure. A slow O-atom tunneling through the singlet–triplet barrier would have the right sort of effect, but this is just much too slow. On the other hand, it is possible there may be some problems with the Wagner–Zabel data.

## Conclusions

It is possible to obtain very precise and likely accurate relaxation times, incubation times, and dissociation rates in  $\text{CO}_2$  using the LS technique. Relaxation gradients are accurately exponential and show consistent  $\tau$  values over a range of

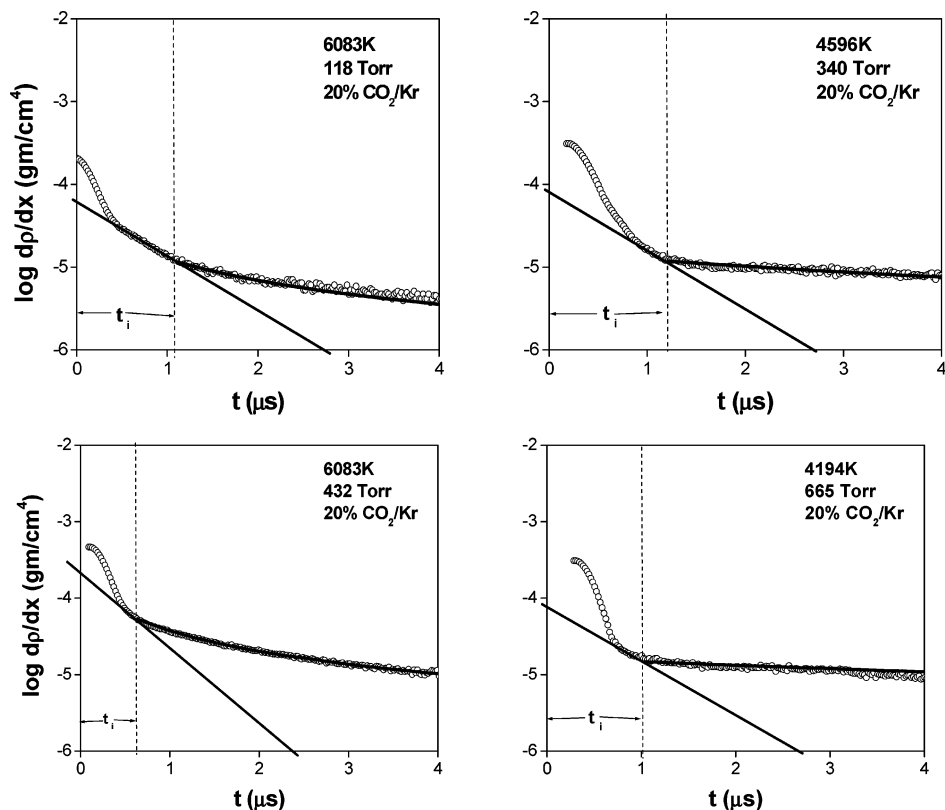


**Figure 7.** Semilog LS profiles used only for dissociation rates. Here incubation times are too short for accurate determination, but the delay they cause is nonetheless recognized. See Figure 6.

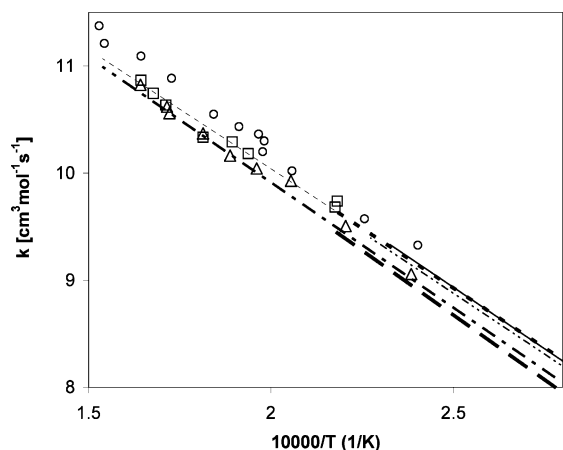


**Figure 8.** Arrhenius plot of second-order rate constants for reaction {1} taken from experiments like those of Figures 6 and 7; [O] 82–190 Torr, [□] 326–432 Torr and [△] 507–750 Torr. Earlier literature rates are listed as follows; [— — —] ref.14, [— · — ·] ref 16, [· · · · ·] ref 17, [thick dashed lines] ref 19, [-----] projection of ref 19, and [—] ref 13.

pressures, and integrated density gradients deviate from thermodynamic calculations in a manner fully consistent with earlier relaxation work. The relaxation is a bit slower than an extrapolation of Simpson's result would suggest, but this may be understood as arising from a lower collision efficiency in Kr than Ar. A slight turning up of the  $\tau$  on the present Landau–Teller plot at the very highest temperatures is nicely explained as a consequence of the rapid rise of the equilibrium vibrational energy at these temperatures. Values for  $\langle \Delta E \rangle_{\text{down}}$ , which have this effect removed, do not show any such rise.

Incubation times were obtained from low-pressure experiments where relaxation and dissociation were both resolved.

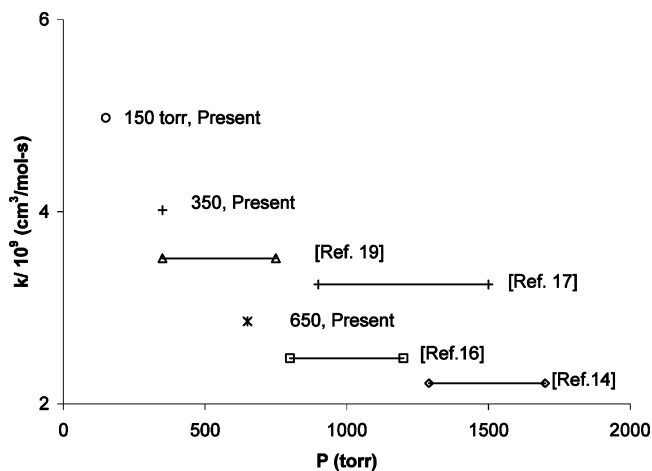


**Figure 9.** Comparison of current and selected recent literature rates as a function of  $P$  for a fixed  $T$  of 4500 K. All these data show very similar variation of rate with  $T$  so the choice of 4500 K is representative. The horizontal lines shown for the literature rates indicate the pressure range apparently used by each experiment. 4500 K is at the high end of the literature studies, so it probably corresponds to the low end of their pressure ranges.

These experiments present relatively long times which should be insensitive to minor time-origin errors. The derived times, expressed as  $t_i/\tau$ , the “time ratio,” drop from 3.4 to 1.3 over  $T = 4000$ – $6600$  K. These values are fully consistent with some earlier theoretical estimates, as well as findings in other species, but are much shorter than those recently reported by Oehlschlaeger et al.<sup>19</sup> These last times imply full vibrational equilibrium during steady reaction and are thus seem inconsistent with second-order dissociation.

**TABLE 2: Gorin-RRKM Model for Reaction:  $\text{CO}_2 \rightarrow \text{CO} + \text{O}$** 

molecular vibration frequencies: 1334, 667(2), 2350  $\text{cm}^{-1}$   
 TS vibration frequency ( $\text{cm}^{-1}$ ): 2170  $\text{cm}^{-1}$   
 external moments of inertia<sup>42</sup>:  $I^+/I = 2.15(E_0/(KT))^{1/3}$   
 TS (active): 1.44858E<sup>-39</sup> gm cm<sup>2</sup> (2)  
 reaction path degeneracy: 2  
 $E_0$  (kcal/mol): 131.7  
 number of Morse oscillators: 1  
 LJ parameters:  $\sigma$  (Å): CO<sub>2</sub>, 3.996; Kr, 3.655.  
 $(\epsilon/k)$  (K): CO<sub>2</sub>, 190; Kr, 178.  $\langle \Delta E \rangle_{\text{down}}$  ( $\text{cm}^{-1}$ ): 44.7( $T/298$ )<sup>1.0</sup>  
 $\eta$  (restriction parameter): 0.999864

Accurate dissociation rates can be obtained from almost all the LS experiments and the results are largely consistent with the most recent literature. They do, however, exhibit one surprise: Over 50–760 Torr, the second-order rate constant actually varies nearly 50%; the reaction is not quite second order. This is actually quite consistent with the best literature data as shown in Figures 8 and 9; all these rate measurements form a much more consistent group if some such small falloff is recognized. However, when a new RRKM calculation, fit to the high-pressure rates of Wagner and Zabel<sup>14</sup> is used to predict behavior under these conditions, this increased falloff is not reproduced. Unfortunately, we have as yet no adequate explanation for the unexpected falloff we have found in this dissociation.

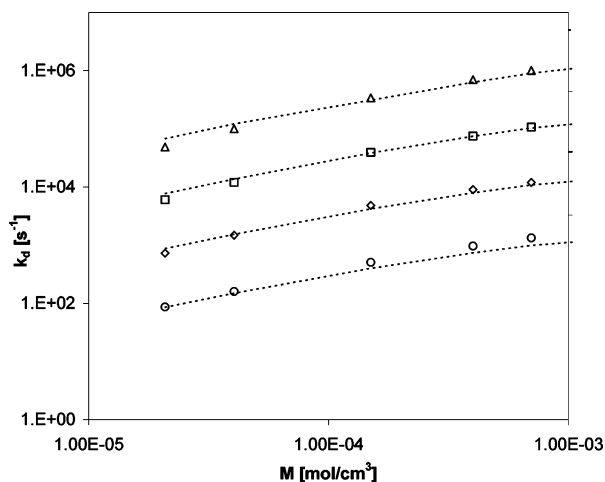


**Figure 10.** Wagner and Zabel<sup>14</sup> rate constants in the high-pressure falloff region: [○] 3000, [◇] 3400, [□] 3900, and [△] 4600 K, with present [----] RRKM-Gorin model fits at these temperatures.

**Acknowledgment.** S.S. and J.K. were supported by the U.S. Department of Energy, Office of Basic Energy Sciences, Division of Chemical Sciences, Geosciences, and Biosciences under Grant No. DE-FE-85ER13384. R.S.T. was supported by the same agency under Contract No. W-31-109-Eng-38. We thank S. J. Klippenstein and L. B. Harding for helpful discussion.

## References and Notes

(1) Burcat, A.; Ruscic, B. *Third Millennium Ideal Gas and Condensed Phase Thermochemical Database for Combustion with updates from Active Thermochemical Tables*; Argonne National Laboratory; Argonne, IL, 2005.

- (2) Buenker, R. J.; Honigmann, M.; Liebermann, H. P. *J. Chem. Phys.* **2000**, *113* (3), 1046.  
 (3) Braunstein, M.; Duff, J. W. *J. Chem. Phys.* **2000**, *112* (6), 2736.  
 (4) The 5.9 kcal/mol barrier value is taken from electronic structure calculations at the ccsd (t)/aug-cc-pvqz/ccsd (t)/aug-cc-pvtz level, using zpe corrections obtained at the ccsd (t)/aug-cc-pvtz level; corrections that appear converged. Harding, L. B. Private communication.  
 (5) Michel, K. W.; Olschewski, H. A.; Richtering, H.; Wagner, H. Gg. *Z. Phys. Chem. N. F.* **1963**, *39*, 129.  
 (6) Davies, W. O. *J. Chem. Phys.* **1964**, *41*, 1846.  
 (7) Davies, W. O. *J. Chem. Phys.* **1965**, *43*, 2809.  
 (8) Michel, K. W.; Olschewski, H. A.; Richtering, H.; Wagner, H. Gg. *Z. Phys. Chem. N. F.* **1965**, *44*, 160.  
 (9) Fishburne, E. S.; Bilwakesh, K. R.; Edse, J. *J. Chem. Phys.* **1966**, *45*, 160.  
 (10) Olschewski, H. A.; Troe, J.; Wagner, H. Gg. *Ber. Bunsen-Ges. Phys. Chem.* **1966**, *70*, 1060.  
 (11) Olschewski, H. A.; Troe, J.; Wagner, H. Gg. *Symp. Int. Combust. Proc.* **1967**, *11*, 155.  
 (12) Dean, A. M. *J. Chem. Phys.* **1973**, *58*, 5202.  
 (13) Hardy, W. A.; Vasatko, H.; Wagner, H. Gg.; Zabel, F. *Ber. Bunsen-Ges. Phys. Chem.* **1974**, *78*, 76.  
 (14) Wagner, H. Gg.; Zabel, F. *Ber. Bunsen-Ges. Phys. Chem.* **1974**, *78*, 705.  
 (15) Brabbs, T. A.; Belles, F. E.; Zlatarich, S. A. *J. Chem. Phys.* **1963**, *38*, 1939.  
 (16) Kiefer, J. H. *J. Chem. Phys.* **1974**, *61*, 244.  
 (17) Burmeister, M.; Roth, P. *AIAA J.* **1990**, *28*, 402.  
 (18) Fujii, N.; Sagawai, S.; Sato, T.; Nosaka, Y.; Miyama, H. *J. Phys. Chem.* **1989**, *93*, 5474.  
 (19) Oehlschlaeger, M. A.; Davidson, D. F.; Jeffries, J. B.; Hanson, R. K. *Z. Phys. Chem.* **2005**, *219*, 555.  
 (20) Generalov, N. A.; Losev, S. A. *J. Quant. Spectrosc. Radiat. Trans.* **1966**, *6*, 101.  
 (21) Galakitinov, I. I.; Korovkina, T. D. *High Temp. (Engl. Transl.)* **1969**, *7*, 1128.  
 (22) Ebrahim, N. A.; Sandeman, R. J. *J. Chem. Phys.* **1976**, *65*, 3446.  
 (23) Clark, T. C.; Dean, A. M.; Kistiakowsky, G. B. *J. Chem. Phys.* **1971**, *54* (4), 1726.  
 (24) Simpson, C. J. S. M.; Bridgeman, K. P.; Chandler, T. R. D. *J. Chem. Phys.* **1968**, *49*, 513.  
 (25) Simpson, C. J. S. M.; Chandler, T. R. D. *Proc. R. Soc. London, Ser. A.* **1970**, *317*, 265.  
 (26) Simpson, C. J. S. M.; Chandler, T. R. D.; Strawson, A. C. *J. Chem. Phys.* **1969**, *51*, 2214.  
 (27) Simpson, C. J. S. M.; Gait, P. D. *Chem. Phys. Lett.* **1977**, *47*, 133.  
 (28) Weaner, D.; Roach, J. F.; Smith, W. R. *J. Chem. Phys.* **1967**, *47*, 3096.  
 (29) Tsang, W.; Kiefer, J. H. *Unimolecular Reactions of Large Polyatomics Molecules Over Wide Ranges of Temperature*; Advance Series in Physical Chemistry 6 (Chemical Dynamics and Kinetics of Small Radicals, Pt.1); World Scientific: River Edge, NJ, 1995; p 58.  
 (30) Forst, W.; Penner, A. P. *J. Chem. Phys.* **1980**, *72*, 1435.  
 (31) Yau, A. U.; Pritchard, H. O. *Can. J. Chem.* **1979**, *57*, 1723.  
 (32) Kiefer, J. H.; Al-Alami, M. J.; Hajduk, J. C. *Appl. Optics* **1981**, *20*, 221.  
 (33) Srinivasan, N. K.; Kiefer, J. H.; Tranter, R. S. *J. Phys. Chem.* **2003**, *107*, 1532.  
 (34) Kiefer, J. H.; Manson, A. C. *Rev. Sci. Instrum.* **1981**, *52*, 1392.  
 (35) Kiefer, J. H.; Kumaran, S. S.; Sundaram, S. *J. Chem. Phys.* **1993**, *99*, 3531.  
 (36) Gardiner, W. C.; Hidaka, Y.; Tanzawa, T. *Combust. Flame* **1981**, *40*, 213.  
 (37) Cottrell T. L.; McCoubrey, J. C. *Molecular Energy Transfer in Gases*; Butterworths: London, 1961.  
 (38) Srinivasan, N. K.; Kiefer, J. H.; Tranter, R. S. *J. Phys. Chem. A* **2001**, *107*, 1532.  
 (39) Dove, J. E.; Teitlebaum, H. *Chem. Phys.* **1974**, *6*, 431.  
 (40) Gebert, Eng. A.; Goos, E.; Hippler, H.; Kachiani, C. *Phys. Chem. Chem. Phys.* **2002**, *4*, 3989.  
 (41) Kiefer, J. H.; Kumaran, S. S. *J. Phys. Chem.* **1993**, *97*, 414; Kiefer, J. H.; Santhanam, S.; Srinivasan, N. K.; Tranter, R. S.; Klippenstein, S. J.; Oehlschlaeger, M. A. *Proc. Combust. Inst.* **2005**, *30*, 1129.  
 (42) Gorin, E. *Acta Physicochim. U. R. S. S.* **1938**, *9*, 5681. Baldwin, A. C.; Golden, D. M. *J. Phys. Chem.* **1978**, *82*, 644.